

OBSERVATION OF THE $^{12}\text{C}(^3\text{He},\pi^+)^{15}\text{N}$ REACTION NEAR THRESHOLD USING RECOIL DETECTION*

W. Schott, W. Wagner, and P. Kienle†

Physik Department der Technischen Universität München, Garching, West Germany

R. Pollock, R. Bent, M. Fatyga, and, J. Kehayias§
Indiana University Cyclotron Facility, Bloomington, Indiana 47405

M. Green and K. Rehm
Argonne National Laboratory, Argonne, Illinois 60439-4843

Analysis of the data from this experiment was completed during 1986. The recoil method for measuring the very small ($^3\text{He},\pi^+$) cross section has been described in previous IUCF Annual Reports.^{1,2} We summarize here the final results.

The experiments were done using the QQSP magnetic spectrometer with a special heavy-ion detector array in the focal plane. The position and direction of the recoil ions at the focal plane were measured by two arrays of transmission-type position-sensitive parallel-plate avalanche counters (PPAC) 29 cm long and 9 cm high. The first detector was located in the spectrograph focal plane, while the second was 10 cm behind the focal plane. The narrow time burst of the IUCF beam, in combination with the fast timing signals from the PPAC array, allowed the ion time-of-flight through the spectrometer (about 100 ns) to be measured with a time resolution of better than 1 ns. By dividing the recoil ion momentum to charge ratio (p/Q), determined from the focal plane position, by the ion velocity, determined from the ion time-of-flight through the spectrometer, the ion mass to charge ratio (A/Q) could be determined with a resolution of about 1%. The atomic number Z of the recoil ion was determined by measuring the energy loss in a gas proportional counter with an area of $29 \times 4 \text{ cm}^2$ mounted immediately behind the second PPAC.

Figure 1 shows a scatter plot of the recoil events as a function of their direction angle (α) and mass-to-charge (A/Q) ratio determined from the ion time-of-flight through the spectrometer. The expected

location of $^{15}\text{N}^{7+}$ ions ($A/Q = 2.143$) is marked in the Figure. No ^{15}N events appear in this display because the threshold for events displayed was set at 2 in order to highlight the mass resolution.

Figure 2 shows the number of events as a function of A/Q and the window that was used for selection of $^{15}\text{N}^{7+}$ ions.

Figure 3 shows the specific energy loss, as deduced from the proportional counter signal, as a function of the inverse velocity of the ion between the target and the first PPAC. The window shown in Figure 2 was used as a condition on the events shown in Figure 3. One notes a weak group of particles with the largest energy loss, which is assigned to ^{15}N . The figure contains a substantial number of less heavily ionizing ^{13}C particles, which originate from ^3He induced spallation reactions. The Z identification does not completely separate this ^{13}C background from the ^{15}N events of interest. To guide the placement of the window separating these two species, the Bethe-Bloch energy loss formula was used with empirical constants adjusted by fitting measured energy loss spectra for more prolific and cleanly identified Be, B and C spallation products.

Figure 4 shows a scatter plot of ^{15}N recoils as a function of their emission angle θ and relative momentum p/p_0 . This plot was made with sorting conditions requiring $A/Q = 2.143$ and $Z = 7$ to be satisfied, as indicated by the windows shown in Figures 2 and 3. These data were taken in a 10-hour run with an average beam current of 60 particle nanoamps. The

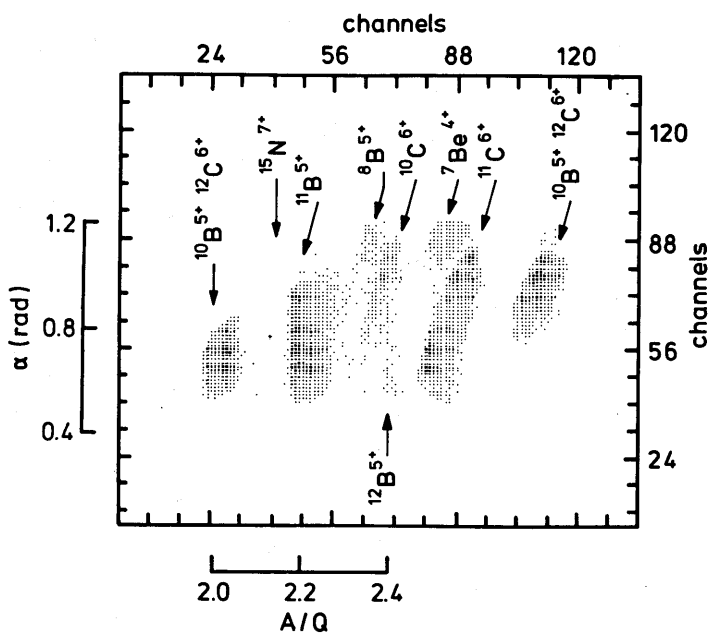


Figure 1. A scatter plot showing reaction products resulting from the bombardment of a ^{12}C target by 181.4 MeV ^3He particles. The coordinates are nominal mass-to-charge ratio (A/Q) and arrival angle (α) of the ions at the spectrograph focal plane. The quantity A/Q is derived from the ion position in the focal plane and flight time through the spectrograph, corrected for path length variation. Prominent groups are labelled by ion species. The threshold for the events displayed is 2.

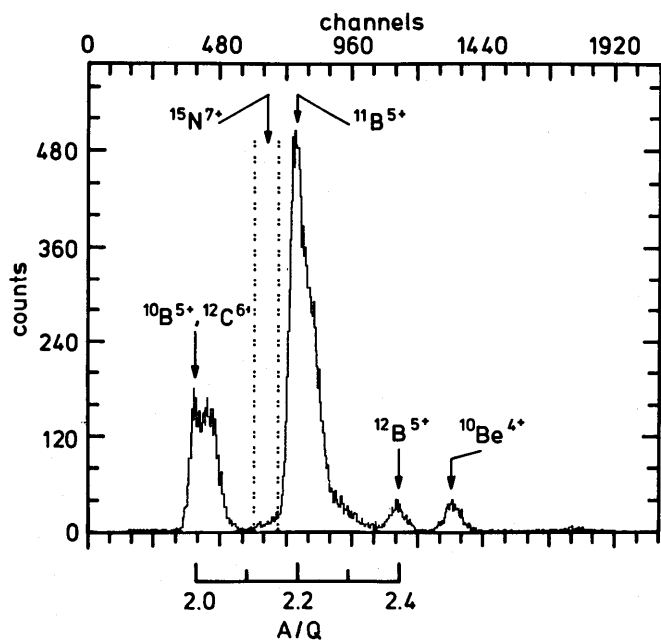


Figure 2. Number of events versus A/Q . The window shows the location of $^{15}\text{N}^{7+}$ ($A/Q = 2.143$) events.

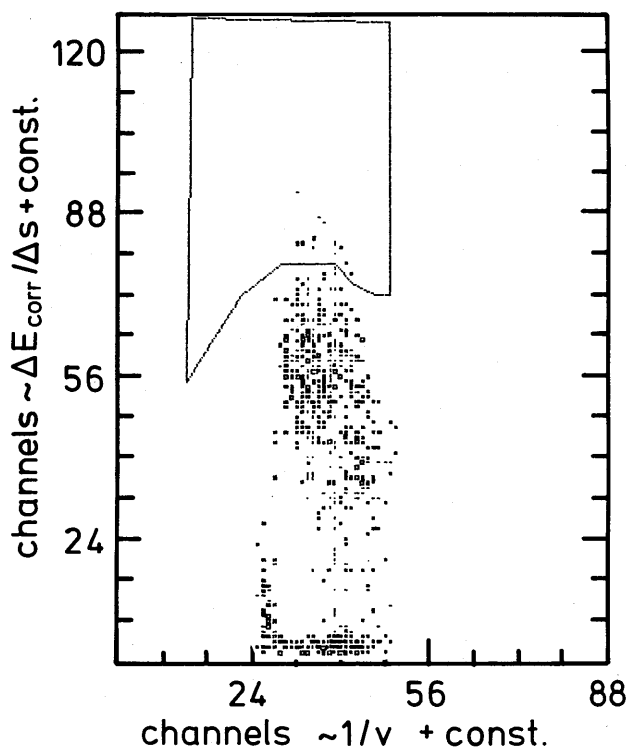


Figure 3. A scatter plot showing a second independent identification of nuclear charged Z . The proportional counter signal amplitude, corrected for path length in the active depth of the counter, is plotted against the flight time within the spectrometer also corrected for path length. The threshold for the events displayed is two. The dependence of dE/ds on velocity gives peaked lines. The events shown are selected from within the window in Fig. 2. The window here shows the location of ^{15}N events. The more prolific, smaller $\Delta E/\Delta s$ events are due to ^{13}C and ^{11}B .

solid elliptical curve is the predicted kinematic locus for ^{15}N fusion products from the $^{12}\text{C}(^3\text{He}, \pi^+)^{15}\text{N}$ reaction leading to the ground state of ^{15}N . Most of the observed events are concentrated on an elliptical locus lying inside the ground state locus, indicating that excited states are more strongly excited than the ground state. The events are concentrated somewhat on the low momentum side, indicating that the reaction favors small angle pion emission, since high recoil momentum is reached with a boost from backward pion emission.

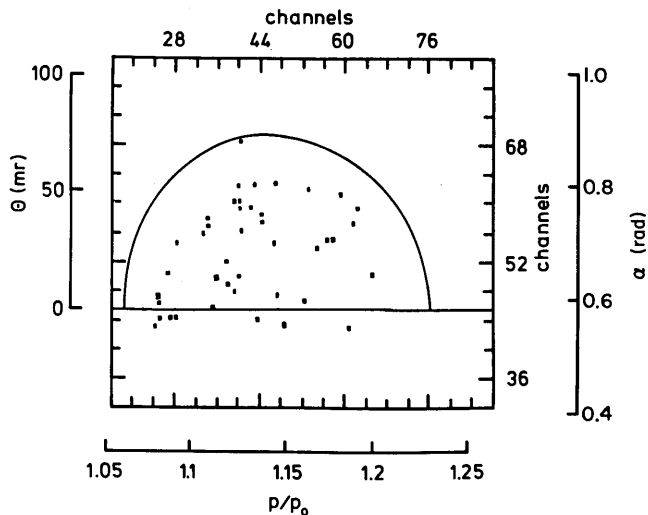


Figure 4. A scatter plot of focal plane position transformed into the relative momentum p/p_0 versus angle of emission at the target, from which longitudinal and transverse momentum per unit charge (p/Q) can be deduced. The reference rigidity of the particles is $p_0/Q = 0.422$ Tesla-meters. The events are selected by the windows shown in Figures 2 and 3. The kinematic locus of ground state events from the $^{12}\text{C}(^3\text{He}, \pi^+)^{15}\text{N}$ reaction is shown by the solid curve.

The solid curve in Figs. 5(a) and 5(b) is a histogram of the number of events as a function of the ^{15}N excitation energy, as derived from the events in Figure 4 by dividing the phase space area into corresponding excitation energy bins. Most of the counts can be attributed to an unresolved group of excited states between 6.5 and 10.5 MeV. The apparent formation of states above 10.4 MeV excitation, an energy region where all known states of ^{15}N are particle unstable with very small gamma branching ratios, can be explained in the following way. The emission angle θ was determined using the radial angle α at the focal plane, ignoring the axial angle ϕ , which could be measured only roughly due to the small angular magnification of 0.3 and large aberrations in this direction. Events with large ϕ , therefore, appear at a too small θ in Figure 4 and are attributed to too large an excitation energy (E_x) in Figure 5. Thus, the distribution of events for a single excited state has a

sharp rise at the energy of the excited state followed by a tail extending into the higher excitation energy region with a sharp kinematic cut-off at $E_x=19$ MeV, as shown by the dotted line in Fig. 5(a), which has been normalized to include the same area as the solid line. We conclude that most of the counts corresponding to $E_x = 13-19$ MeV in Fig. 5 are due to this effect. Adding these events to those in the $E_x = 6.5-10.5$ MeV region increases the cross section by a factor of 1.6, leading to an angle-integrated cross section of 1.3 ± 0.3 nb for this group. For calculating the cross section, an experimentally determined recoil detection efficiency of 0.84 was applied.

A recent study³ of the $^{12}\text{C}(^3\text{He}, \pi^+)^{15}\text{N}$ reaction at a considerably higher bombarding energy of 235 MeV showed a similar enhancement of the yield to states

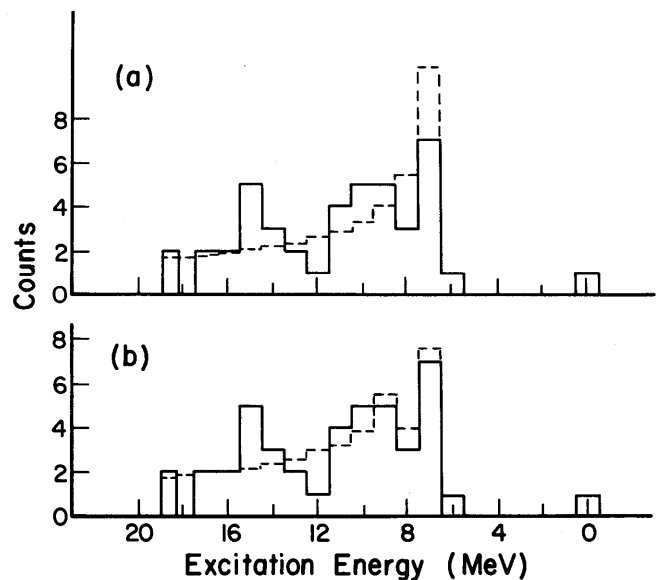


Figure 5. Solid lines: the distribution of ^{15}N events by excitation energy in ^{15}N , summed over all pion emission angles. Dotted lines: (a) fit to the data assuming population of a single state at an excitation energy of 6.5 MeV; (b) fit to the data assuming population of two states at excitation energies of 6.5 and 8.5 MeV with relative populations of 0.7 and 0.3, respectively.

above 6 MeV, and a comparable magnitude for the cross section. The Orsay results³ indicate strong population of two groups of states centered around 6.5 and 8.5 MeV. A slightly improved fit to the distribution of events in Fig. 5 can be achieved by assuming population of these two groups of excited states with relative probabilities of 0.7 and 0.3, respectively, as shown by the dotted line in Fig. 5(b).

There are too few events in Fig. 4 to determine reliably the angular distribution of the differential cross section for population of the group of states between 6.5 and 10.5 MeV excitation energy. The events shown in Fig. 4 suggest a fairly isotropic angular distribution, with perhaps some peaking in the forward direction.

In summary, we have shown that the extremely small yield pionic fusion process $^{12}\text{C}(^3\text{He}, \pi^+)^{15}\text{N}$ can be observed close to threshold by detection of the ^{15}N

recoil ions. The kinematic projection of the recoil ions into a forward cone gives this technique unusually high efficiency. At 181.4 MeV bombarding energy, the angle integrated cross section for production of excited states in ^{15}N between 6.5 and 10.5 MeV is 1.3 ± 0.3 nb. The ground state of ^{15}N is very weakly populated. The pion angular distribution for the strong group is peaked somewhat in the forward direction.

*This work was supported in part by a grant from the Bundesministerium fur Forschung und Technologie.

†Present address: GSI, Darmstadt, West Germany.

§Present address: Brookhaven National Laboratory, Long Island, NY 11973

- 1) R.D. Bent et al., IUCF Scientific and Technical Report, p. 90 (1983).
- 2) J. Homulka et al., IUCF Scientific and Technical Report, p.23 (1985).
- 3) L. Bimbot et al., Phys. Rev. C 30 739 (1984).

A MICROSCOPIC MODEL OF THE (p, π) REACTION

P.W.F. Alons and R.D. Bent
Indiana University Cyclotron Facility, Bloomington, Indiana 47405

J.S. Conte
Indiana University Cyclotron Facility, Bloomington, Indiana 47405
and Purdue University Computing Center, West Lafayette, Indiana 47907

M. Dillig
Institute for Theoretical Physics, University of Erlangen-Nurnberg, Erlangen, W. Germany

The purpose of this work is to develop the capability for reliable (p, π) calculations based on a realistic, microscopic meson-exchange model of the $A(p,\pi)A+1$ reaction in the form of a thoroughly tested computer code that is fast and flexible with regard to nuclear structure and other physics input.

Our model includes both the one-nucleon mechanism (ONM), in which the pion is produced directly from the

projectile in a stripping- or bremsstrahlung-like process (Fig. 1a), and the resonant p-wave rescattering part of the two-nucleon mechanism (TNM), in which the pion is produced in a single "hard" collision between the incident proton and one target nucleon (Fig. 1b). Effects due to "soft" proton-nucleus and pion-nucleus interactions before and after the production process are included via local mean-field corrections